HHS Public Access

Author manuscript

Chem Eng J. Author manuscript; available in PMC 2020 June 24.

Published in final edited form as:

Chem Eng J. 2019 May 15; 364: 428–439. doi:10.1016/j.cej.2019.01.175.

Efficient H_2O_2 electrogeneration at graphite felt modified via electrode polarity reversal: Utilization for organic pollutants degradation

Wei Zhou[a,b], **Ljiljana Rajic**[c], **Xiaoxiao Meng**[a], **Roya Nazari**[b], **Yuwei Zhao**[b], **Yan Wang**[a], **Jihui Gao**[a,*], **Yukun Qin**[a], **Akram N. Alshawabkeh**[b,*]

[a]School of Energy Science and Engineering, Harbin Institute of Technology, Harbin 150001, P. R. China;

[b]Department of Civil and Environmental Engineering, Northeastern University, Boston, Massachusetts 02115, United States;

[c]Pioneer Valley Coral and Natural Science Institute, 1 Mill Valley Road, Hadley, MA 01035, USA

Abstract

Electrochemical synthesis of H_2O_2 offers a great potential for water treatment. However, a significant challenge is the development of efficient cathode materials for the process. Herein, we implement a practical electrochemical cathode modification to support efficient H_2O_2 electrogeneration via the reduction of dissolved anodic O_2. Graphite felt (GF) is *in situ* anodically modified by electrode polarity reversal technique in an acid-free, low-conductivity electrolyte. The modified GF exhibits a significantly higher activity towards O_2 reduction. Up to 183.3% higher H_2O_2 yield is obtained by the anodized GF due to the increased concentrations of oxygen-containing groups and the hydrophilicity of the surface, which facilitates electron and mass transfer between GF and the electrolyte. Another significant finding is the ability to produce H_2O_2 at a high yield under neutral pH and low current intensity by the modified GF (35% of the charge need to produce the same amount by unmodified GF). Long-term stability testing of the modified GF showed a decay in the electrode's activity for H_2O_2 production after 30 consecutive applications. However, the electrode regained its optimal activity for H_2O_2 production after a secondary modification by electrode polarity reversal. Finally, *in situ* electrochemically modified GF is more effective for removal of reactive blue 19 (RB19, 20 mg/L) and ibuprofen (IBP, 10 mg/L) by the electro-Fenton process. The modified GF removed 62.7% of RB19 compared to only 28.1% by the unmodified GF in batch reactors after 50 min. Similarly, 75.3% IBP is removed by the modified GF compared to 57.6% by the unmodified GF in a flow-through reactor after 100 min.

[*]**Corresponding author**: Prof. Jihui Gao, School of Energy Science and Engineering, Harbin Institute of Technology, 92, Dazhi Street, Nangang District, Harbin 150001, China, gaojh@hit.edu.cn; Akram N. Alshawabkeh, PhD, PE, Fellow ASCE, George A. Snell Professor of Engineering, Department of Civil and Environmental Engineering, Northeastern University, 360 Huntington Avenue, Boston, MA 02115, a.alshawabkeh@neu.edu.

Graphical Abstract

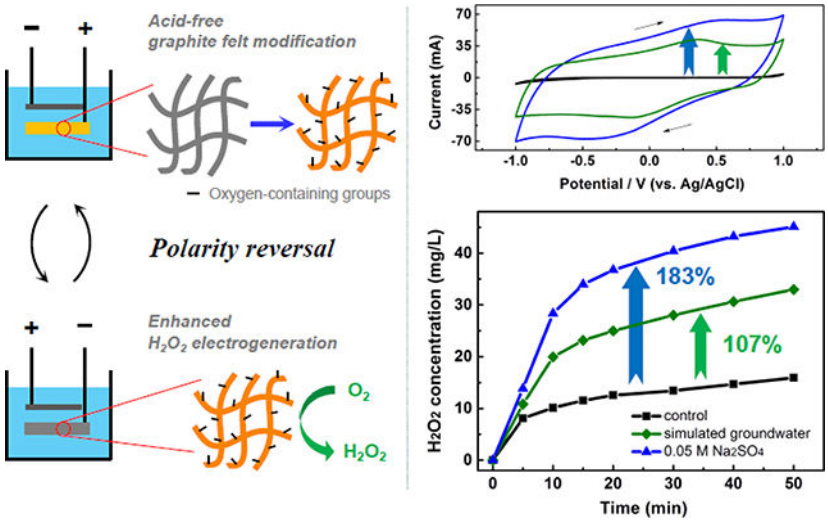

Keywords

Electro-Fenton; Graphite felt; Hydrogen peroxide; Hydroxyl radicals; Oxygen-containing group

1. Introduction

Advanced methods for efficient and sustainable treatment of surface and groundwater are of great interest [1][2]. The electro-Fenton (EF) reaction is a viable advanced oxidation process (AOPs) for water treatment that has gained interest in recent decades [3][4][5][6]. In this process, H_2O_2 is electrochemically generated at the cathode by 2-electron reduction of oxygen (Eq. 1), coupled with the regeneration of Fe^{2+} at the same electrode (Eq. 2). The process allows for efficient and sustained *in situ* generation of H_2O_2 and avoids the challenges of chemicals transportation, storage of H_2O_2, and the formation of iron sludge [7][8].

$$O_2 + 2H^+ + 2e^- \rightarrow H_2O_2 (0.695\ \text{V}\ vs.\ \text{SHE}) \quad (1)$$

$$Fe^{3+} + e^- \rightarrow Fe^{2+} (0.77\ \text{V}\ vs.\ \text{SHE}) \quad (2)$$

The efficiency of H_2O_2 generation is highly dependent on the cathode material and operation parameters [3][9][10][11]. Carbonaceous materials are the most widely used cathodes because they are non-toxic, stable, conductive and chemical resistant [3], exhibit high overpotential of H_2 evolution, and low catalytic activity for H_2O_2 decomposition [12]. To date, graphite [4], graphite felt (GF) [9][12][13][14], carbon felt [15], activated carbon fiber [16], carbon-polytetrafluoroethylene (PTFE) [17], and reticulated vitreous carbon (RVC) [18][19][20] have been used as cathodes for the EF process. However, conventional

carbonaceous materials usually show poor kinetics towards the 2-electron oxygen reduction reaction (ORR) resulting in poor performance for H_2O_2 production.

Significant efforts have been conducted to modify carbonaceous materials to enhance its electrochemical activity towards H_2O_2 generation. Generally, the methods are divided into two types. The first is depositing other catalysts on the surface of carbonaceous materials, such as graphene [21], carbon nanotubes [22][23], acetylene black [24], carbon black [9], and metal oxides (i.e., MnO_2 [25], CeO_2 [26]). The second is heteroatom-doping, such as O [27][28], N [29][30], and F [31]. The introduction of oxygen-containing functional groups (OGs) could induce higher electrical conductivity and electrocatalytic activity due to the formation of a hydrophilic surface [12][32][33]. More importantly, the introduction of OGs at the carbon surface is the most facile and low-cost method to improve the H_2O_2 production via 2-electron ORR [27][28]. The methods to introduce OGs are divided into three categories that are induced by concentrated strong oxidants (H_2O_2 [34], H_2SO_4 [33], and HNO_3 [34]), hydroxyl radicals (generated by Fenton's reagents [35][36]), and electrochemical oxidation [12][33][37][38][39]. However, using strong oxidants or Fenton's reagents is difficult to control for water treatment, even though reagent concentration, reaction time, and temperature are usually regulated in an attempt to impose control [40]. Electrochemical oxidation is the most promising method to introduce OGs to carbon surface since it is practical, controllable and environmentally friendly.

Although considerable research has been conducted to introduce OGs to carbon surface by electrooxidation [34][40][41], less attention has been paid to H_2O_2 production for water treatment by the EF process. Moreover, most of the studies use strong acids [33][38][42] or concentrated salts [39][40] as electrolytes (Table 1), making the process costly, difficult for up-scaling and possibly limiting its potential for *in situ* applications. Barton et al. [40] reported that activated carbon was electrooxidized by anodic treatment in 0.5 M K_2SO_4 electrolyte. Yue et al. [43] electrochemically oxidized carbon fibers in 1% by weight aqueous KNO_3 and over 1 mmol/g of total titratable acidic functional groups were achieved by 6360 C/g electrooxidation extent. Miao et al. [33] treated GF electrochemically in a concentrated H_2SO_4 solution (5, 10, 20% by weight), the O/C ratio reached 0.22 compared to 0.043 for the blank sample.

Electrode polarity reversal is based on defined time intervals of operation under reversed electrode polarity [44]. It is a very practical and controllable process and has been used for electrokinetic remediation of heterogeneous media [44][45]. In soil remediation, pH distribution can be controlled by optimizing the electrode sequence and duration of polarity reversal [45]. In Pd-catalytic EF processes, both H_2 and O_2 could be generated in the Pd catalyst vicinity when reversing the electrode polarity [46]. While this technique was used to control pH and reaction conditions, it has not been evaluated for sequential GF electrode modification and H_2O_2 production in the same reactor for organic pollutants degradation. This method would be practical and very impactful as GF electrodes could be modified *in situ*, thus avoiding the complexity of conventional modification methods. More importantly, the method can be implemented in a second stage to regain the optimal catalytic performance of GF electrodes once a decay on H_2O_2 catalytic generation appears.

The objective of this study is to develop a green and practical electrochemical GF modification method that can operate *in situ* and achieve sequential cathode modification and H_2O_2 generation by electrode polarity reversal. Electrooxidation of GF in low-conductivity, acid-free solutions (50 mM Na_2SO_4 electrolyte, simulated groundwater) is evaluated, for the first time. Various characterization methods were used to reveal the mechanism of the enhanced H_2O_2 yield. The impact of electrolyte pH and current on H_2O_2 generation are assessed. Long-term stability of the modified GF electrode was evaluated by continuous testing for over 1500 min, followed by a second stage of electrode polarity reversal to regain the optimal catalytic performance of the GF electrode. Finally, simultaneous GF electrode modification and H_2O_2 production were evaluated for the transformation of reactive blue 19 (RB19) and ibuprofen (IBP) by the EF process in both a batch reactor and flow-through reactor.

2. Materials and methods

2.1 Chemicals and materials

All chemicals in this study were analytical grade and used as received. Sodium sulfate (anhydrous, ≥99%), titanium sulfate (99.9%), and reactive blue 19 (RB19, 99%) were purchased from Sigma-Aldrich. Ibuprofen (2-(4-(2-methyl propyl)phenyl)propanoic acid, $C_{13}H_{18}O_2$) was obtained from Fisher Scientific. Deionized water (18.2 MΩ cm) obtained from a Millipore Milli-Q system was used in all the experiments. Solution pH was adjusted by sulfuric acid (98%, JT Baker) and sodium hydroxide (Fisher Scientific). GF (≥99%, 2cm×4cm×3.2mm, mass of 0.25 g, Fuel Cell Store) and Ti/mixed metal oxide (MMO, 3N International) mesh were selected as electrode materials (Figure S1). GF is one of the commonly used carbonaceous materials in the EF process and the vanadium redox flow battery due to good stability, conductivity, and commercial availability [38]. Its physical characteristics are shown in Figure S2. The Ti/MMO electrode consists of IrO_2 and Ta_2O_5 coating on a titanium mesh with dimension of 3.6 cm diameter by 1.8 mm thickness.

2.2 Experimental design

An undivided electrochemical batch reactor was used for H_2O_2 generation and GF modification. (Figure 1). The oxygen was *in situ* supplied by the Ti/MMO anode because oxygen supplied by external pure O_2 or air aeration usually achieves an extremely low O_2/air utilization efficiency (<0.1%) [48]. An electrolyte of 50 mM Na_2SO_4 or a simulated groundwater that consists of 5 mM Na_2SO_4 and 0.3 mM $CaSO_4$ [49] were used. For electrochemical modification, the GF electrode served as an anode while the Ti/MMO electrode served as a cathode. The polarity reversal (PR) allowed further H_2O_2 electrogeneration by using a PR device (DPDT relay, Omron, H3CR-F8-300AC-100/240). Constant currents were applied by an Agilent E3612A DC power supply. GF modified in 50 mM Na_2SO_4 electrolyte under current of “X” mA for “Y” min are denoted as GF-X-Y. GF modified in simulated groundwater under current of “X” mA for “Y” min are denoted as GF-X-Y-GW.

Different levels of electrooxidation were achieved by altering the current intensity and oxidation time. The applied charge was 0, 480, 960, 1440 and 1920 C/g (charge per gram

electrode). H_2O_2 electrogeneration by the modified GF was investigated in a batch reactor. The EF process was enabled by simultaneous GF modification and H_2O_2 production and was applied for transformation of anthraquinone dye RB19 and anti-inflammatory drug ibuprofen (IBP) in 50 mM Na_2SO_4 electrolyte (batch reactor) and simulated groundwater (flow-through reactor, shown in Figure S3), respectively.

2.3 Characterization of the modified GF

The surface morphology was characterized by scanning electron microscopy (SEM, Hitachi SU-8000). The surface OGs were analyzed by X-ray photoelectron spectroscopy (XPS) analysis on a PHI 5700 ESCA system and were also analyzed by NaOH uptake methods (Section S1) [40][43]. The contact angle was measured by a contact angle meter (OCA15, Dataphysics). Cyclic voltammetry (CV), linear sweep voltammetry (LSV), and chronoamperometry (CA) were carried out in a three-electrode cell system at room temperature to evaluate the activity and stability of modified GF for H_2O_2 generation. The prepared GF cathode was used as the working electrode, a platinum plate (1cm×1cm) as counter electrode and a Ag/AgCl electrode as the reference electrode, the data were recorded by a SP-300 electrochemical workstation (BioLogic, France).

2.4 Analytical and calculation methods

At specific times, a 3 mL solution sample was collected to measure H_2O_2 concentration at 405 nm by a Shimazu UV-Vis spectrometer after coloration with $TiSO_4$ [46]. The concentration of RB19 was measured using the same instrument at 592 nm. pH and dissolved oxygen (DO) were measured by a pH meter and a DO meter (Thermo Scientific). Benzoic acid (BA) has a high second-order rate constant with hydroxyl radicals (4.2×10^9 M^{-1} s^{-1}) [50] and can be used for semi-quantitative determination of hydroxyl radicals [51]. The fluorescence intensity of product was measured by fluorescence spectrophotometer (Shimadzu XRF-1800) at an excitation wavelength of 303 nm.

Ibuprofen was measured by a 1200 Infinity Series HPLC (Agilent) equipped with a 1260 diode array detector (DAD), a 1260 fluorescence detector (FLD) and an Agilent Eclipse AAA C18 column (4.6×150 mm). The mobile phase was a mixture of methanol and water (68:32, v/v) at the flow rate of 0.5 mL/min. The detection wavelengths for DAD was set at 282 nm, and the column temperature at 40 °C [52][53]. Total organic carbon (TOC) was determined using a TOC-5050 Shimadzu analyzer.

The current efficiency (CE) for H_2O_2 generation, defined as the ratio of the electricity consumed by the electrode reaction over the total electricity passed through the circuit, is calculated by Eq. 3. Where n is the number of electrons transferred for O_2 reduction to H_2O_2, F is the Faraday constant (96,486 C mol^{-1}), C_{H2O2} is the concentration of H_2O_2 (mol L^{-1}), V is the electrolyte volume (L), I is the applied current intensity (A), and t is the reaction time (s). The removal efficiency of RB19 and IBP (η) is calculated using Eq.4, where C_0 and C_t are the concentration of chemical at time zero and time t, respectively.

$$CE = \frac{nFC_{H_2O_2}V}{\int_0^t Idt} \times 100\% \quad (3)$$

$$\eta = \frac{C_0 - C_t}{C_0} \times 100\% \quad (4)$$

3. Results and discussion

3.1 Characterization

3.1.1 Electrochemical characterization—CV and LSV were carried out on unmodified and modified GF to investigate whether electrochemical oxidation in acid-free, low-conductivity electrolyte could enhance the electrocatalytic activity of GF toward ORR (Figure 2). The current response of GF dramatically increased after electrooxidation (Figure 2(a)). The best current response was observed after 30 min treatment (GF-200–30) and the response decreased under a longer treatment time of 40 min. A similar electrooxidation level (charge of 1440 C/g) was also achieved by a lower current (50 mA) and a longer time (120 min), which produced a higher current response than the unmodified GF (Figure S4). The LSV curve measured in a N_2 saturated solution shows an extremely low current before −1.2 V. The current then significantly increases with the negative shift of potential, indicating the occurrence of the hydrogen evolution reaction (HER) (Eq. 5) [54]. The inner figure in Figure 2(b) shows that the modified GF exhibits higher ORR activity in the following order: GF-200–30 > GF-200–40 > GF-200–20 > GF-200–10. Further, the hydrogen evolution potential of the modified GF electrodes shifts to less negative, indicating that ORR and HER activity were simultaneously enhanced. This reflects that the ability to enhance H_2O_2 generation could compete with H_2 evolution reaction on the modified GF cathode (discussed further in Section 3.2).

$$2H_2 + 2e^- \rightarrow H_2 \quad (5)$$

Results of the chronoamperometry test (Figure2(c)) show that after 36000 s continuous run, a 8.4% decay was observed for the GF-200–30 electrode, indicating that the modified GF electrode exhibits a good reproducibility and good cycling stability. This is very beneficial to sustain a stable H_2O_2 yield for several sequential operations.

3.1.2 XPS analysis—The content of surface OGs of the GF electrode before and after modification were first measured by NaOH uptake method (Table S1). The total mass of the OGs increased by more than 25 times: from 17.3 μmol/g by the unmodified GF to 445.4 μmol/g after modification under 200 mA for 30 min. This indicates that electrooxidation in acid-free (50 mM Na_2SO_4) electrolyte introduces acidic OGs to the GF electrode surface. Although increasing the processing time from 10 to 30 min under 200 mA increased the content of functional groups, further modification to 40 min severely decreased the content of these groups. This is caused by mineralization of active site atoms on the graphite felt

surface; active sites are oxidized to form OGs such as C-OH, C=O and finally CO_2 (a simplified step-wise progression mechanism has been widely studied and presented in Eq. 6 [43][55]).

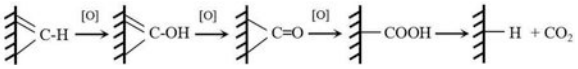

(6)

Even in simulated groundwater with extremely low conductivity, 192.1 μmol/L oxygen-containing groups were introduced. The mass of OGs that are formed in our work is not as high as in those reported by electrooxidation conducted in strong acids or concentrated salts solutions [12][56]. Typical results are shown in Table S2.

To further identify the surface elements, the XPS wide scan spectra in the binding energy range of 0–1350 eV was obtained for the unmodified GF and GF-200–30 (Figure 3a). The peaks for carbon and oxygen are centered at around 284 and 532 eV, respectively. The O/C ratio (calculated by the peak area of O1s and C1s) increased from 0.055 for the unmodified GF to 0.218 for GF-200–30, demonstrating the significant effect of the electrochemical modification. Peak fitting of C1s and O1s were carried out to identify the functional groups and the respective percentage. The results are shown in Figure 3(b)~(f). For the C1s spectra (Figure 3(b) and (c)), the main peak at 284.6–284.7 eV is attributed to graphitized carbon (C=C), the other 3 peaks could be attributed to defects on the GF surface (C-C, 285.1 eV), C-OH (286.0–286.3 eV), C=O (287.7–288.2 eV) [36][57]. For the O1s spectra (Figure 3(d) and (e)), the peaks at 531.0–531.1 eV, 532.2–532.7 eV, 533.9–534.2 eV, could be assigned to C=O, −OH, and the adsorbed molecular H_2O, respectively. The relative content of each surface groups is calculated based on the peak areas, and results are summarized in Table 2. The content of C=O and C-OH significantly increased from 5.91% to 14.93% and from 10.52% to 19.41%, respectively. It was reported [27][58] that OGs facilitate the 2-electron ORR for H_2O_2 generation. Thus, after electrochemical modification, more active sites are expected to support a more efficient H_2O_2 production.

3.1.3 SEM and contact angle measurement—Figure 4 shows the SEM images and contact measurements of the unmodified sample, GF modified in 50 mM Na_2SO_4 under 200 mA for 30 min, and GF modified in simulated groundwater under 200 mA for 30 min, respectively. The GF is composed of an entangled network of carbon micro filaments [32]. After electrooxidation in 50 mM Na_2SO_4 or in simulated groundwater, the morphology of GF did not significantly change. However, flaky structures are observed on the modified carbon micro filaments (marked with yellow arrows). Contact angle measurements show that the unmodified GF electrode is hydrophobic, while the modified GF electrode exhibits excellent hydrophilic properties (Figure 4). Samples modified in 50 mM Na_2SO_4 are more hydrophilic in that droplets disappear after 0.5 s. This property is significant for H_2O_2 electrogeneration, which determines the electron transfer and mass transfer of dissolved oxygen from electrolyte to active sites on the electrode surface [32][59]. The photo in Figure 4(g) also clearly demonstrated that the unmodified GF is hydrophobic and the modified GF is highly hydrophilic. Therefore, the highly improved hydrophilic property of the GF surface

will drastically enhance the electron transfer and mass transfer of electrolyte and GF cathode, generating more H_2O_2, as discussed later.

3.2 H_2O_2 electrogeneration

3.2.1 Drastically enhanced H_2O_2 production by the modified GF—A constant current of 200 mA was applied for different modification durations to anodize the GF electrode in 50 mM Na_2SO_4 electrolyte using the setup shown in Figure 1. After electrochemical modification, the GF electrode was used as a cathode to test its performance for H_2O_2 generation. Profiles of H_2O_2 concentration are shown in Figure 5(a). Figure 5(b) shows the relationship between voltage and current for the original and modified GF electrodes, and the inner figure shows the correlation between H_2O_2 concentration at 60 min and the contents of OGs.

All modified GF electrodes show better activity compared with the original GF. Within 30 min, the higher the electrooxidation, the higher the production of H_2O_2. After 60 min, the anodized GF electrode produced 45.1 mg/L H_2O_2, nearly 2.9 times higher than the original GF. The increased yield of H_2O_2 production is due to the enhanced current response to ORR, which is in accordance with the CV, LSV, and contents of functional groups results shown in Figure 2(a), Figure 2(b), and Figure 3, respectively. However, further modification duration causes a decrease in H_2O_2 yields (Eq. 6) [43][55]. Differences in the kinetics of H_2O_2 generation were identified. For GF-200–30, the concentration of H_2O_2 tends to increase over time up to 60 min, while for GF-200–40, it reaches a steady state after 20 min with a gradual decrease in *CE* (Figure S5). This can be caused by simultaneous H_2O_2 generation and decomposition. H_2O_2 can be decomposed under several pathways, such as disproportion (Eq. 7) [3][60], cathodic reduction (Eq. 8) [3][60], and anodic oxidation (Eq. 9) [3][61] in bulk electrolyte. With the gradual increased concentration of H_2O_2, its decomposition also emerges, limiting the kinetics of H_2O_2 generation.

$$2\,H_2O_2 \rightarrow O_2(g) + 2\,H_2O(\text{Bulk electrolyte and cathode vicinity}) \tag{7}$$

$$H_2O_2 + 2\,H^+ + 2e^- \rightarrow 2\,H_2O(\text{Cathode surface and inside, 1.77 V } \textit{vs}\,.\ \text{SHE}) \tag{8}$$

$$H_2O_2 \rightarrow HO_2\cdot + H^+ + e^-(\text{Anode surface}) \tag{9–1}$$

$$HO_2\cdot \rightarrow O_2(g) + H^+ + e^-(\text{Anode surface}) \tag{9–2}$$

Moreover, a much lower voltage was required for the same current for the modified GF electrode compared with that of the unmodified electrode (Figure 5(b)). Under 100 mA, the voltage decreased from 4.23 V to 3.10 V. The decreased cell voltage leads to a lower power and the potential for a cost-effective EF process.

The highest H_2O_2 production was obtained by electrochemical modification under 200 mA for 30 min (electrooxidation charge of 1440 C/g). The influence of different time and current

combinations under the same electrooxidation rate on H_2O_2 generation is shown in Figure S6. Although the same charge is applied, the H_2O_2 yield significantly decreased when lowering the current; 35.7 mg/L H_2O_2 was measured using the GF electrode that was modified under 100 mA for 60 min, while just 8.9 mg/L H_2O_2 was measured for the same electrode under 50 mA for 120 min. These results demonstrate that there is an optimum current level for the formation of oxygen-containing groups to the GF surface.

3.2.2 Influence of pH and current—The influence of electrolyte pH and current on the performance of the modified GF electrode in a 0.5 M Na_2SO_4 electrolyte was investigated (Figure 6). To the best of our knowledge, for the first time, we found the pH has a completely different impact on the performance of the modified and unmodified GF electrode. For the unmodified GF electrode, pH significantly impacts H_2O_2 generation. A significantly higher concentration of H_2O_2 was formed under acidic conditions, up to 32.4 mg/L under pH of 2.08, compared to neutral pH (16.8 mg/L at pH 7) and alkaline conditions (15.5 mg/L at pH 11). These differences are consistent with the literature [62][63]; under acidic conditions, enough protons are available for 2-electron ORR to produce H_2O_2 while under alkaline conditions, surface OGs are neutralized by OH^-, reducing 2-electron ORR activity as well as H^+ production at the anode. Furthermore, H_2O_2 decomposes faster under pH 10 [7].

After modification, GF showed superior performance for H_2O_2 generation under both neutral and acidic conditions (Figure 6(a)). H_2O_2 generation severely decreased at pH 11. The influence of H^+ on H_2O_2 generation rate can be ascribed to the enhanced H_2 evolution reaction (HER, Eq. 5) on the modified GF electrode (Figure 2(b)). Thus, the influence of increased H^+ reduction to H_2 at lower pH was nonnegligible on the competition of electrons with 2-electron ORR reaction for H_2O_2 generation. CV curves of unmodified and modified GF electrodes in different pHs are shown in Figure S7.

The H_2O_2 concentration within the initial 15 min decreases with decreasing current (Figure 6(b)) as follows: 200 mA > 150 mA > 100 mA > 50 mA. This is due to increasing current response toward ORR when applying a higher current. However, competing reactions also increase with increasing current. When the competing processes that cause depletion of H_2O_2 (Eq. 7~9) exceed the generation of H_2O_2, the H_2O_2 concentration in solution decreases. For the modified GF electrode (see Figure 6(b)), H_2O_2 generation under 50 mA achieved almost the same yield under 100 mA after 50 min (45.1 and 45.4 mg/L, respectively), while 200 mA and 150 mA produced less H_2O_2 yield. Higher current may also cause significant decomposition of H_2O_2, by mechanisms such as anodic oxidation (Eq. 9) and cathodic reduction (Eq. 8). The results show that the highest H_2O_2 yield can be obtained at neutral pH and under low currents, which has the potential to lower costs and simplify applications and maintenance.

3.3 Application of the modification strategy in simulated groundwater

The feasibility of this green modification method in groundwater is important. This will allow simultaneous GF modification and EF reaction in practice. Simulated groundwater that consists of 5 mM Na_2SO_4 and 0.3 mM $CaSO_4$ was used as an electrolyte for

modification. The influence of electrolyte pH and current were then carried out to evaluate the performance of H_2O_2 electrogeneration.

Comparisons of GF modified in 50 mM Na_2SO_4 and simulated groundwater are shown in Figure 7(a). The voltage required for different currents is shown in Figure 7(b). The modified GF electrode generated 33.0 mg/L H_2O_2 after 50 min, compared to 45.1 mg/L for GF electrode modified in 50 mM Na_2SO_4. Although the concentration in simulated groundwater is less than in 50 mM Na_2SO_4, H_2O_2 concentration is 108% higher than concentrations measured by unmodified GF electrodes, demonstrating the successful introduction of OGs to the GF surface.

Moreover, we also find that the GF modified in simulated groundwater requires a lower voltage for the same current. Under 100 mA, the voltage is 14.9% lower with the modified GF than the unmodified GF (3.61 V versus 4.23 V, respectively). The benefit gradually disappears under higher currents. During modification and under 200 mA, the voltage for simulated groundwater (24.0 V) is much higher than for 50 mM Na_2SO_4 electrolyte (5.73 V).

The influence of initial pH and current on H_2O_2 generation by GF electrodes modified in simulated groundwater (Figure 7(c,d)) are similar to those presented in Figure 6(a) and Figure 6(b). Acidic pH and neutral pH exhibit the same tendency for H_2O_2 generation, while pH of 11 reduces H_2O_2 generation. However, for the GF modified electrode in simulated groundwater, the gap between pH of 11 and other pHs is smaller than that for the GF modified in 50 mM Na_2SO_4. This is possibly because there are less oxygen-containing groups in simulated groundwater, and limiting the effect of alkaline conditions on electrode activity toward 2-electron ORR. Further, the carboxylic acid groups might bind with Ca^{2+} in the electrolyte and less −COOH are available for H_2O_2 production [64]. The same applies in 50 mM Na_2SO_4: the highest H_2O_2 production was obtained by 50 mA, while 150 mA and 200 mA caused depletion of H_2O_2.

3.4 Sequential modification and H_2O_2 generation by electrode polarity reversal

Coupled electrochemical modification of GF and H_2O_2 generation is a very promising strategy for the treatment of waste water and groundwater because of lower operation costs and easier maintenance. It is necessary to understand the impact of electrolyte after electrooxidation on H_2O_2 generation. After electrochemical oxidation, the residual electrolyte was used for H_2O_2 generation experiments and the results were summarized in Figure 8(a) and 8(b). The production of H_2O_2 decreased in residual electrolyte both for the modified and unmodified GF electrodes. To examine why organic products of electrooxidation influence H_2O_2 generation, CV curves (Figure 8(b)) were obtained in the residual electrolyte. A new reductive curve is formed in the range of −0.5 to +0.5 V. The peak value increases with the increase of electrolyte TOC, illustrating the reduction of organic products on the electrode. This reaction co-occurs with O_2 reduction reaction, thus competing with H_2O_2 electrogeneration, and resulting in a lower production of H_2O_2 in the residual electrolyte. The nature of these compounds will be investigated in future experiments. The effect of PR frequency on H_2O_2 production is presented in Figure S8.

Generally, with the increase of electrooxidation extent, the electrolyte TOC increases. Electrooxidation is a process that gradually oxidizes carbon to −COH, −COOH, and finally CO_2. In this process, there are some aliphatic acids produced [65][66], which leached into the electrolyte and contribute to the increase of TOC in the solution. As presented in Figure 8(b), the TOC values significantly increase with an increase in charge, up to 79.5 mg/L (GF-200–40). In addition, we observed that polarity reversal induces less TOC changes in the electrolyte, which demonstrate its feasibility for implementation.

3.5 Long-term stability of GF-200–30

Considering that the EF process is developed for long-term and large-scale application, the stability of the cathode with cycling is significant for determining the performance of EF process. Decay of the performance of H_2O_2 production would result in a loss of the precious active materials and an increase in the capital cost for maintenance [67]. Previous work shows acceptable stability for O-doping cathode materials. For example, Lu et al. [27] tested the stability of oxidized carbon nanotubes (CNTs) by chronoamperometric technique and observed a negligible changes in current response. Zhou et al. evaluated the stability of anodized GF electrode for p-nitrophenol degradation in 10-times continuous runs, and the TOC removal efficiency decreased within 15% [12]. However, the running time of these tests are not long enough. Furthermore, electroreduction of carboxyl groups upon negative polarization has been reported in the literature [68], which may impact the H_2O_2 production over long-term operation.

The long-term stability of the GF-200–30 cathode is tested in this study for over 30 cycles. Most importantly, after a decay in H_2O_2 production appears, we implemented a strategy of polarity reversal to assess the potential for *in situ* secondary modification of the GF-200–30 electrode to regain its optimal capacity. After 10 cycles of treatment, H_2O_2 production by the GF-200–30 was maintained at 85.1% (Figure 9) of the initial capacity. After 30 cycles, H_2O_2 production further decreased by 66.4%. It has been reported [68] that a significant amount of unstable oxides could be irreversibly removed with reduction using a cathodic potential sweep. In our case, the OGs such as the carboxyl groups are not stable and its partial reduction could explain the gradual decrease in H_2O_2 production over time. After a second stage modification by polarity reversal (Figure 9), the GF-200–30 regained its capacity for H_2O_2 production. Different from other modification approaches, the electrochemical modification by polarity reversal is powerful in that it can be conducted in situ without additions of chemicals or removal of cathodes from the reactor. This finding is very important as it makes this strategy stand out from various modification approaches.

3.6 Implementation for RB19 and IBP degradation in batch (50 mM Na_2SO_4) and flow-through reactor (simulated groundwater)

This study presents a new strategy to operate GF electrode modification *in situ* for highly efficient H_2O_2 electrogeneration, which is green, practical and easy to scale-up. Here, RB 19 and IBP were used to test the effectiveness of this approach for transformation of chemicals. Experiments were conducted in a batch reactor with 50 mM Na_2SO_4 electrolyte (setup shown in Figure 1) and a 3-electrode flow-through reactor with simulated groundwater (Figure 10(d)), respectively. Results (Figure 10(a) and (b)) demonstrated that EF process

using in-situ electrochemically modified GF is more effective for RB19 and IBP degradation than the unmodified GF (remove efficiency of 62.7% and 28.1% for RB19 in batch reactor at 50 min, 75.3% and 57.6% for IBP in column reactor after 100 min for modified and unmodified GF, respectively). This is consistent with results presented in Figure 5(a), where higher H_2O_2 production was obtained by modified GF cathodes. Furthermore, as Figure 10(c) shows, by using benzoic acid as trapping reagent for ·OH, a higher spectral peak value in EF process with modified GF cathode in batch reactor is obtained, implies that more ·OH are generated, thus inducing a higher removal efficiency. Compared with the literature [69] [70], the removal kinetics of IBP in flow-through reactor could be further enhanced by using external O_2 supply, and increasing Fe^{2+} concentration. This result also implies that the approach presented can be applied to waste water treatment and groundwater remediation using EF process.

4. Conclusions

This work develops a novel electrochemical cathode modification approach to support efficient H_2O_2 electrocatalytic generation via reduction of dissolved anodic O_2. The modified GF exhibits higher activity towards O_2 reduction, which is ascribed to the increased concentrations of oxygen-containing groups and the hydrophilicity of the surface that facilitates electron and mass transfer between electrodes and the electrolyte. H_2O_2 concentration was thus increased from 15.9 mg/L to 45.1 mg/L and 33.0 mg/L in 50 mM Na_2SO_4 and simulated groundwater, respectively. Compared with unmodified electrodes, neutral pH and low current of 50 mA supported effective H_2O_2 generation. Gradually decreased activity of modified GF was observed over 30 continuous cycles, however, the activity could be regained by a secondary modification by electrode polarity reversal. Finally, EF process enabled by *in situ* modified GF via electrode polarity reversal exhibits higher removal efficiency for RB19 and IBP in batch reactor (50 mM Na_2SO_4) and flow-through reactor (simulated groundwater), respectively, proving its great potential practical application for organic waste water treatment and groundwater remediation.

Supplementary Material

Refer to Web version on PubMed Central for supplementary material.

Acknowledgments

This work was financially supported by the US National Institute of Environmental Health Sciences (NIEHS, Grant No. P42ES017198) and National Natural Science Foundation of China (Grant No. 51776055). The content is solely the responsibility of the authors and does not necessarily represent the official views of the NIEHS, the National Institutes of Health and the National Natural Science Foundation of China. Valuable suggestions from Prof. Fei Sun are appreciated by all authors. We also thank China Scholarship Council for the financial support to Wei Zhou.

References

[1]. Pignatello JJ, Oliveros E, MacKay A, Advanced Oxidation Processes for Organic Contaminant Destruction Based on the Fenton Reaction and Related Chemistry, Critical Reviews in Environmental Science and Technology. 36 (2006) 1–84. doi:10.1080/10643380500326564.

[2]. Zhou W, Gao J, Zhao H, Meng X, Wu S, The role of quinone cycle in Fe^{2+}–H_2O_2 system in the regeneration of Fe^{2+}, Environmental Technology. 38 (2017) 1887–1896. doi:10.1080/09593330.2016.1240241. [PubMed: 27734760]

[3]. Sirés I, Brillas E, Oturan MA, Rodrigo MA, Panizza M, Electrochemical advanced oxidation processes: Today and tomorrow. A review, Environmental Science and Pollution Research. 21 (2014) 8336–8367. doi:10.1007/s11356-014-2783-1. [PubMed: 24687788]

[4]. Wang CT, Hu JL, Chou WL, Kuo YM, Removal of color from real dyeing wastewater by Electro-Fenton technology using a three-dimensional graphite cathode, Journal of Hazardous Materials. 152 (2008) 601–606. doi:10.1016/j.jhazmat.2007.07.023. [PubMed: 17707581]

[5]. Nidheesh PV, Gandhimathi R, Trends in electro-Fenton process for water and wastewater treatment: An overview, Desalination. 299 (2012) 1–15. doi:10.1016/j.desal.2012.05.011.

[6]. Umar M, Aziz HA, Yusoff MS, Trends in the use of Fenton, electro-Fenton and photo-Fenton for the treatment of landfill leachate, Waste Management. 30 (2010) 2113–2121. doi:10.1016/j.wasman.2010.07.003. [PubMed: 20675113]

[7]. Qiang ZM, Chang JH, Huang CP, Electrochemical generation of hydrogen peroxide from dissolved oxygen in acidic solutions, Water Research. 36 (2002) 85–94. doi:10.1016/S0043-1354(01)00235-4. [PubMed: 11766820]

[8]. Chen L, Ma J, Li X, Zhang J, Fang J, Guan Y, Xie P, Strong enhancement on Fenton oxidation by addition of hydroxylamine to accelerate the ferric and ferrous iron cycles, Environmental Science and Technology. 45 (2011) 3925–3930. doi:10.1021/es2002748. [PubMed: 21469678]

[9]. Yu F, Zhou M, Yu X, Cost-effective electro-Fenton using modified graphite felt that dramatically enhanced on H_2O_2 electro-generation without external aeration, Electrochimica Acta. 163 (2015) 182–189. doi:10.1016/j.electacta.2015.02.166.

[10]. Daneshvar N, Aber S, Vatanpour V, Rasoulifard MH, Electro-Fenton treatment of dye solution containing Orange II: Influence of operational parameters, Journal of Electroanalytical Chemistry. 615 (2008) 165–174. doi:10.1016/j.jelechem.2007.12.005.

[11]. Scialdone O, Galia A, Gattuso C, Sabatino S, Schiavo B, Effect of air pressure on the electro-generation of H_2O_2 and the abatement of organic pollutants in water by electro-Fenton process, Electrochimica Acta. 182 (2015) 775–780. doi:10.1016/j.electacta.2015.09.109.

[12]. Zhou L, Zhou M, Zhang C, Jiang Y, Bi Z, Yang J, Electro-Fenton degradation of p-nitrophenol using the anodized graphite felts, Chemical Engineering Journal. 233 (2013) 185–192. doi:10.1016/j.cej.2013.08.044.

[13]. Zhou W, Gao J, Kou K, Meng X, Wang Y, Ding Y, Xu Y, Zhao H, Wu S, Qin Y, Highly efficient H_2O_2 electrogeneration from O_2 reduction by pulsed current: Facilitated release of H_2O_2 from porous cathode to bulk, Journal of the Taiwan Institute of Chemical Engineers. 83 (2018) 59–63. doi:10.1016/j.jtice.2017.10.041.

[14]. Zhou W, Meng X, Rajic L, Xue Y, Chen S, Ding Y, Kou K, Wang Y, Gao J, Qin Y, Alshawabkeh AN, "Floating" cathode for efficient H_2O_2 electrogeneration applied to degradation of ibuprofen as a model pollutant, Electrochemistry Communications. (2018). doi:10.1016/J.ELECOM.2018.09.007.

[15]. Pimentel M, Oturan N, Dezotti M, Oturan MA, Phenol degradation by advanced electrochemical oxidation process electro-Fenton using a carbon felt cathode, Applied Catalysis B: Environmental. 83 (2008) 140–149. doi:10.1016/j.apcatb.2008.02.011.

[16]. Wang A, Qu J, Ru J, Liu H, Ge J, Mineralization of an azo dye Acid Red 14 by electro-Fenton's reagent using an activated carbon fiber cathode, Dyes and Pigments. 65 (2005) 227–233. doi:10.1016/j.dyepig.2004.07.019.

[17]. Isarain-Chávez E, Arias C, Cabot PL, Centellas F, Rodríguez RM, Garrido JA, Brillas E, Mineralization of the drug β-blocker atenolol by electro-Fenton and photoelectro-Fenton using an air-diffusion cathode for H_2O_2 electrogeneration combined with a carbon-felt cathode for Fe^{2+} regeneration, Applied Catalysis B: Environmental. 96 (2010) 361–369. doi:10.1016/j.apcatb.2010.02.033.

[18]. Li Q, Batchelor-Mcauley C, Lawrence NS, Hartshorne RS, V Jones CJ, Compton RG, A flow system for hydrogen peroxide production at reticulated vitreous carbon via electroreduction of

oxygen, Journal of Solid State Electrochemistry. 18 (2014) 1215–1221. doi:10.1007/s10008-013-2250-9.

[19]. Zhou W, Gao J, Ding Y, Zhao H, Meng X, Wang Y, Kou K, Xu Y, Wu S, Qin Y, Drastic enhancement of H_2O_2 electro-generation by pulsed current for ibuprofen degradation: Strategy based on decoupling study on H_2O_2 decomposition pathways, Chemical Engineering Journal. 338 (2018) 709–718. doi:10.1016/j.cej.2017.12.152. [PubMed: 32153347]

[20]. Zhou W, Rajic L, Zhao Y, Gao J, Qin Y, Alshawabkeh AN, Rates of H_2O_2 electrogeneration by reduction of anodic O_2 at RVC foam cathodes in batch and flow-through cells, Electrochimica Acta. 277 (2018) 185–196. doi:10.1016/j.electacta.2018.04.174. [PubMed: 32153302]

[21]. Yang W, Zhou M, Cai J, Liang L, Ren G, Jiang L, Ultrahigh yield of hydrogen peroxide on graphite felt cathode modified with electrochemically exfoliated graphene, J. Mater. Chem. A 5 (2017) 8070–8080. doi:10.1039/C7TA01534H.

[22]. Khataee AR, Safarpour M, Zarei M, Aber S, Electrochemical generation of H_2O_2 using immobilized carbon nanotubes on graphite electrode fed with air: Investigation of operational parameters, Journal of Electroanalytical Chemistry. 659 (2011) 63–68. doi:10.1016/j.jelechem.2011.05.002.

[23]. Babaei-Sati R, Basiri Parsa J, Electrodeposition of PANI/MWCNT nanocomposite on stainless steel with enhanced electrocatalytic activity for oxygen reduction reaction and electro-Fenton process, New J. Chem 41 (2017) 5995–6003. doi:10.1039/C7NJ00744B.

[24]. Sheng Y, Zhao Y, Wang X, Wang R, Tang T, Electrogeneration of H_2O_2 on a composite acetylene black-PTFE cathode consisting of a sheet active core and a dampproof coating, Electrochimica Acta. 133 (2014) 414–421. doi:10.1016/j.electacta.2014.04.071.

[25]. Aveiro LR, da Silva AGM, Antonin VS, Candido EG, Parreira LS, Geonmonond RS, de Freitas IC, Lanza MRV, Camargo PHC, Santos MC, Carbon-supported MnO_2 nanoflowers: Introducing oxygen vacancies for optimized volcano-type electrocatalytic activities towards H_2O_2 generation, Electrochimica Acta. 268 (2018) 101–110. doi:10.1016/j.electacta.2018.02.077.

[26]. Assumpção MHMT, Moraes A, De Souza RFB, Reis RM, Rocha RS, Gaubeur I, Calegaro ML, Hammer P, V Lanza MR, Santos MC, Degradation of dipyrone via advanced oxidation processes using a cerium nanostructured electrocatalyst material, Applied Catalysis A: General. 462–463 (2013) 256–261. doi:10.1016/j.apcata.2013.04.008.

[27]. Lu Z, Chen G, Siahrostami S, Chen Z, Liu K, Xie J, Liao L, Wu T, Lin D, Liu Y, Jaramillo TF, Nørskov JK, Cui Y, High-efficiency oxygen reduction to hydrogen peroxide catalysed by oxidized carbon materials, Nature Catalysis. (2018). doi:10.1038/s41929-017-0017-x.

[28]. Kim HW, Ross MB, Kornienko N, Zhang L, Guo J, Yang P, McCloskey BD, Efficient hydrogen peroxide generation using reduced graphene oxide-based oxygen reduction electrocatalysts, Nature Catalysis. 1 (2018) 282–290. doi:10.1038/s41929-018-0044-2.

[29]. Fellinger TP, Hasché F, Strasser P, Antonietti M, Mesoporous nitrogen-doped carbon for the electrocatalytic synthesis of hydrogen peroxide, Journal of the American Chemical Society. 134 (2012) 4072–4075. doi:10.1021/ja300038p. [PubMed: 22339713]

[30]. Sun Y, Sinev I, Ju W, Bergmann A, Dresp S, Kühl S, Spöri C, Schmies H, Wang H, Bernsmeier D, Paul B, Schmack R, Kraehnert R, Roldan Cuenya B, Strasser P, Efficient Electrochemical Hydrogen Peroxide Production from Molecular Oxygen on Nitrogen-Doped Mesoporous Carbon Catalysts, ACS Catalysis. 8 (2018) 2844–2856. doi:10.1021/acscatal.7b03464.

[31]. Zhao K, Su Y, Quan X, Liu Y, Chen S, Yu H, Enhanced H_2O_2 production by selective electrochemical reduction of O_2 on fluorine-doped hierarchically porous carbon, Journal of Catalysis. 357 (2018) 118–126. doi:10.1016/j.jcat.2017.11.008.

[32]. Zhou L, Zhou M, Hu Z, Bi Z, Serrano KG, Chemically modified graphite felt as an efficient cathode in electro-Fenton for p-nitrophenol degradation, Electrochimica Acta. 140 (2014) 376–383. doi:10.1016/j.electacta.2014.04.090.

[33]. Miao J, Zhu H, Tang Y, Chen Y, Wan P, Graphite felt electrochemically modified in H_2SO_4 solution used as a cathode to produce H_2O_2 for pre-oxidation of drinking water, Chemical Engineering Journal. 250 (2014) 312–318. doi:10.1016/j.cej.2014.03.043.

[34]. Berenguer R, Marco-Lozar JP, Quijada C, Cazorla-Amorós D, Morallón E, Effect of electrochemical treatments on the surface chemistry of activated carbon, Carbon. 47 (2009) 1018–1027. doi:10.1016/j.carbon.2008.12.022.

[35]. Li W, Bai Y, Zhang Y, Sun M, Cheng R, Xu X, Chen Y, Mo Y, Effect of hydroxyl radical on the structure of multi-walled carbon nanotubes, Synthetic Metals. 155 (2005) 509–515. doi:10.1016/j.synthmet.2005.07.346.

[36]. Gao C, Wang N, Peng S, Liu S, Lei Y, Liang X, Zeng S, Zi H, Influence of Fenton's reagent treatment on electrochemical properties of graphite felt for all vanadium redox flow battery, Electrochimica Acta. 88 (2013) 193–202. doi:10.1016/j.electacta.2012.10.021.

[37]. Tang X, Guo K, Li H, Du Z, Tian J, Electrochemical treatment of graphite to enhance electron transfer from bacteria to electrodes, Bioresource Technology. 102 (2011) 3558–3560. doi:10.1016/j.biortech.2010.09.022. [PubMed: 20888221]

[38]. Zhang W, Xi J, Li Z, Zhou H, Liu L, Wu Z, Qiu X, Electrochemical activation of graphite felt electrode for VO^{2+}/VO2+ redox couple application, Electrochimica Acta. 89 (2013) 429–435. doi:10.1016/j.electacta.2012.11.072.

[39]. Pittman CU, Jiang W, Yue ZR, Gardner S, Wang L, Toghiani H, Leon Y Leon CA, Surface properties of electrochemically oxidized carbon fibers, Carbon. 37 (1999) 1797–1807. doi:10.1016/S0008-6223(99)00048-2.

[40]. Barton SS, Evans MJB, Halliop E, MacDonald JAF, Anodic Oxidation of Porous Carbon, Langmuir. 13 (1997) 1332–1336. doi:10.1021/la9509413.

[41]. Yoon CM, Long D, Jang SM, Qiao W, Ling L, Miyawaki J, Rhee CK, Mochida I, Yoon SH, Electrochemical surface oxidation of carbon nanofibers, Carbon. 49 (2011) 96–105. doi:10.1016/j.carbon.2010.08.047.

[42]. Li X, Huang K, Liu S, Tan N, Chen L, Characteristics of graphite felt electrode electrochemically oxidized for vanadium redox battery application, Transactions of Nonferrous Metals Society of China (English Edition). 17 (2007) 195–199. doi:10.1016/S1003-6326(07)60071-5.

[43]. Yue ZR, Jiang W, Wang L, Gardner SD, Pittman CU, Surface characterization of electrochemically oxidized carbon fibers, Carbon. 37 (1999) 1785–1796. doi:10.1016/S0008-6223(99)00047-0.

[44]. Rajic L, Fallahpour N, Yuan S, Alshawabkeh AN, Electrochemical transformation of trichloroethylene in aqueous solution by electrode polarity reversal, Water Research. 67 (2014) 267–275. doi:10.1016/j.watres.2014.09.017. [PubMed: 25282093]

[45]. Pazos M, Sanromán MA, Cameselle C, Improvement in electrokinetic remediation of heavy metal spiked kaolin with the polarity exchange technique, Chemosphere. 62 (2006) 817–822. doi:10.1016/j.chemosphere.2005.04.071. [PubMed: 15970309]

[46]. Yuan S, Fan Y, Zhang Y, Tong M, Liao P, Pd-catalytic in situ generation of H_2O_2 from H_2 and O_2 produced by water electrolysis for the efficient electro-fenton degradation of rhodamine B., Environmental Science & Technology. 45 (2011) 8514–20. doi:10.1021/es2022939. [PubMed: 21866953]

[47]. Tabti Z, Ruiz-Rosas R, Quijada C, Cazorla-Amorós D, Morallón E, Tailoring the Surface Chemistry of Activated Carbon Cloth by Electrochemical Methods., ACS Applied Materials & Interfaces. 6 (2014) 11682–11691. doi:10.1021/am502475v. [PubMed: 24955482]

[48]. Yu F, Zhou M, Zhou L, Peng R, A Novel Electro-Fenton Process with H_2O_2 Generation in a Rotating Disk Reactor for Organic Pollutant Degradation, Environmental Science and Technology Letters. 1 (2014) 320–324. doi:10.1021/ez500178p.

[49]. Mao X, Yuan S, Fallahpour N, Ciblak A, Howard J, Padilla I, Loch-Caruso R, Alshawabkeh AN, Electrochemically induced dual reactive barriers for transformation of TCE and mixture of contaminants in groundwater, Environmental Science and Technology. 46 (2012) 12003–12011. doi:10.1021/es301711a. [PubMed: 23067023]

[50]. Liang C, Su HW, Identification of sulfate and hydroxyl radicals in thermally activated persulfate, Industrial and Engineering Chemistry Research. 48 (2009) 5558–5562. doi:10.1021/ie9002848.

[51]. G. S and Ananthakrishnan R, Semi-Quantitative Determination of Hydroxyl Radicals by Benzoic Acid Hydroxylation: An Analytical Methodology for Photo-Fenton Systems, Current Analytical Chemistry. 8 (2012) 143–149. doi:10.2174/157341112798472297.

[52]. Yuan S, Gou N, Alshawabkeh AN, Gu AZ, Efficient degradation of contaminants of emerging concerns by a new electro-Fenton process with Ti/MMO cathode, Chemosphere. 93 (2013) 2796–2804. doi:10.1016/j.chemosphere.2013.09.051. [PubMed: 24125716]

[53]. Xiang Y, Fang J, Shang C, Kinetics and pathways of ibuprofen degradation by the UV/chlorine advanced oxidation process, Water Research. 90 (2016) 301–308. doi:10.1016/j.watres.2015.11.069. [PubMed: 26748208]

[54]. Xia G, Lu Y, Xu H, Electrogeneration of hydrogen peroxide for electro-Fenton via oxygen reduction using polyacrylonitrile-based carbon fiber brush cathode, Electrochimica Acta. 158 (2015) 390–396. doi:10.1016/j.electacta.2015.01.102.

[55]. Horie K, Hiromichi M, Mita I, Bonding of epoxy resin to graphite fibres, Fibre Science and Technology. 9 (1976) 253–264. doi:10.1016/0015-0568(76)90008-7.

[56]. Pittman CU, Jiang W, Yue ZR, Leon y Leon CA, Surface area and pore size distribution of microporous carbon fibers prepared by electrochemical oxidation, Carbon. 37 (1999) 85–96. doi:10.1016/S0008-6223(98)00190-0.

[57]. Wang Y, Liu Y, Wang K, Song S, Tsiakaras P, Liu H, Preparation and characterization of a novel KOH activated graphite felt cathode for the electro-Fenton process, Applied Catalysis B: Environmental. 165 (2015) 360–368. doi:10.1016/j.apcatb.2014.09.074.

[58]. Basova YV, Hatori H, Yamada Y, Miyashita K, Effect of oxidation–reduction surface treatment on the electrochemical behavior of PAN-based carbon fibers, Electrochemistry Communications. 1 (1999) 540–544. doi:10.1016/S1388-2481(99)00112-5.

[59]. Sheng Y, Song S, Wang X, Song L, Wang C, Sun H, Niu X, Electrogeneration of hydrogen peroxide on a novel highly effective acetylene black-PTFE cathode with PTFE film, Electrochimica Acta. 56 (2011) 8651–8656. doi:10.1016/j.electacta.2011.07.069.

[60]. Sánchez-Sánchez CM, Bard AJ, Hydrogen peroxide production in the oxygen reduction reaction at different electrocatalysts as quantified by scanning electrochemical microscopy, Analytical Chemistry. 81 (2009) 8094–8100. doi:10.1021/ac901291v. [PubMed: 19725556]

[61]. Özcan A, Şahin Y, Koparal AS, Oturan MA, A comparative study on the efficiency of electro-Fenton process in the removal of propham from water, Applied Catalysis B: Environmental. 89 (2009) 620–626. doi:10.1016/j.apcatb.2009.01.022.

[62]. Sirés I, Brillas E, Remediation of water pollution caused by pharmaceutical residues based on electrochemical separation and degradation technologies: A review, Environment International. 40 (2012) 212–229. doi:10.1016/j.envint.2011.07.012. [PubMed: 21862133]

[63]. Zhang C, Fan FRF, Bard AJ, Electrochemistry of oxygen in concentrated NaOH solutions: Solubility, diffusion coefficients, and superoxide formation, Journal of the American Chemical Society. 131 (2009) 177–181. doi:10.1021/ja8064254. [PubMed: 19063634]

[64]. Bala T, V Prasad BL, Sastry M, Kahaly MU, V Waghmare U, Interaction of different metal ions with carboxylic acid group: a quantitative study., The Journal of Physical Chemistry. A 111 (2007) 6183–6190. doi:10.1021/jp067906x. [PubMed: 17585841]

[65]. Gong X, Wang M, Wang Z, Guo Z, Roles of inherent mineral matters for lignite water slurry electrolysis in H_2SO_4 system, Energy Conversion and Management. 75 (2013) 431–437. doi:10.1016/j.enconman.2013.07.004.

[66]. Seehra MS, Bollineni S, Nanocarbon boosts energy-efficient hydrogen production in carbon-assisted water electrolysis, International Journal of Hydrogen Energy. 34 (2009) 6078–6084. doi:10.1016/j.ijhydene.2009.06.023.

[67]. Zhao TS, Jiang HR, Shyy W, Zeng L, Zhang RH, Highly efficient and ultra-stable boron-doped graphite felt electrodes for vanadium redox flow batteries, Journal of Materials Chemistry A. (2018) 1–10. doi:10.1039/c6ta03804b.

[68]. Cheng PZ, Teng H, Electrochemical responses from surface oxides present on HNO3-treated carbons, Carbon. 41 (2003) 2057–2063. doi:10.1016/S0008-6223(03)00212-4.

[69]. Loaiza-Ambuludi S, Panizza M, Oturan N, Özcan A, Oturan MA, Electro-Fenton degradation of anti-inflammatory drug ibuprofen in hydroorganic medium, Journal of Electroanalytical Chemistry. 702 (2013) 31–36. doi:10.1016/j.jelechem.2013.05.006.

[70]. Skoumal M, Rodríguez RM, Cabot PL, Centellas F, Garrido JA, Arias C, Brillas E, Electro-Fenton UVA photoelectro-Fenton and solar photoelectro-Fenton degradation of the drug

ibuprofen in acid aqueous medium using platinum and boron-doped diamond anodes, Electrochimica Acta. 54 (2009) 2077–2085. doi:10.1016/j.electacta.2008.07.014.

Highlights

1. A novel and green cathode modification by electrode polarity reversal was first reported.
2. Increase in surface oxygen-containing groups and hydrophilic properties were observed.
3. For modified electrode, low current and neutral pH could support the highest H_2O_2 yield.
4. The modified graphite felt cathode exhibited good reproducibility and longevity.
5. Modified cathode in column reactor supported ibuprofen removal from simulated groundwater.

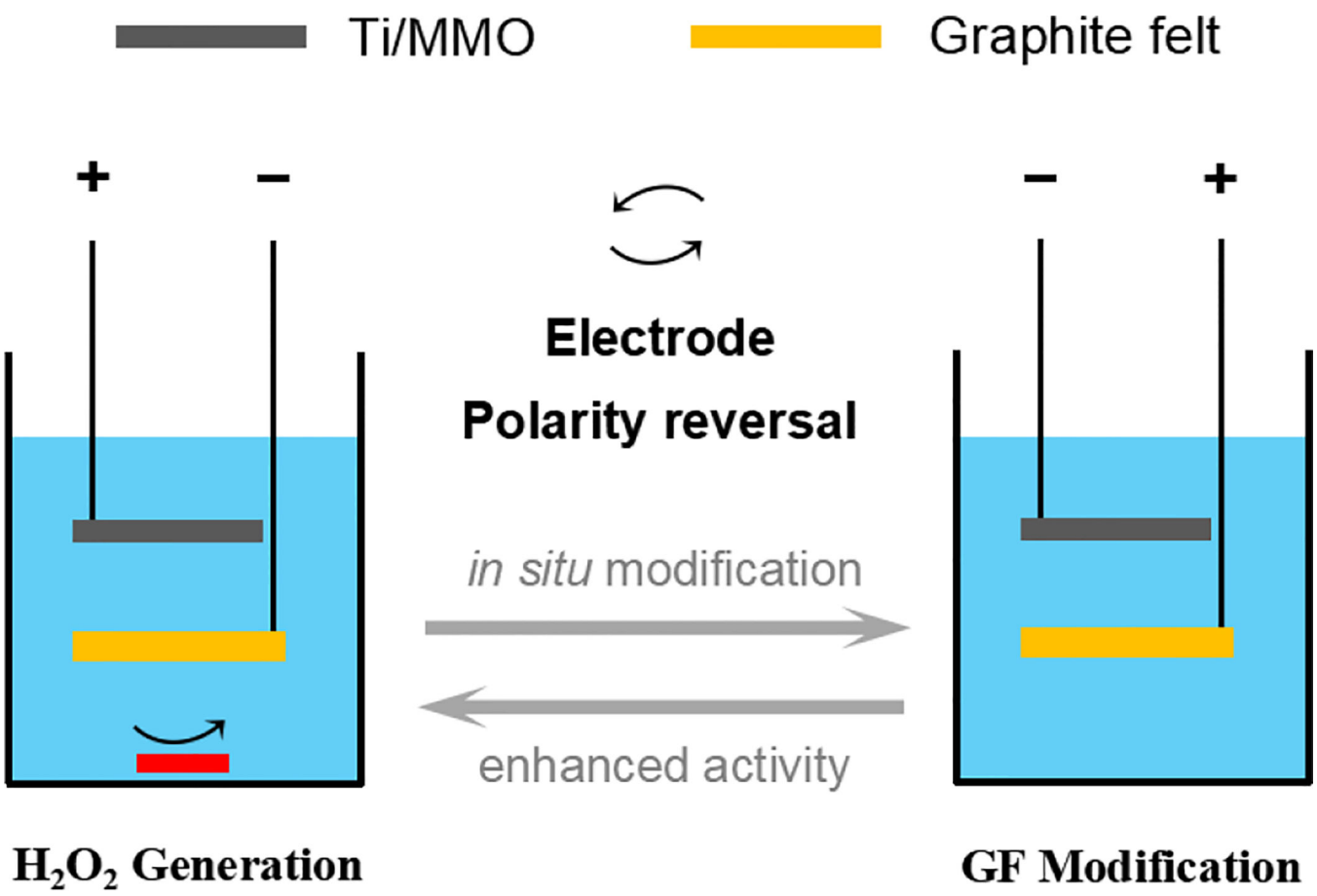

Figure 1.
Schematic diagram of sequential GF modification and H_2O_2 generation by electrode polarity reversal in a batch reactor. Ti/MMO electrode was arranged above the GF electrode with a distance of 3 cm.

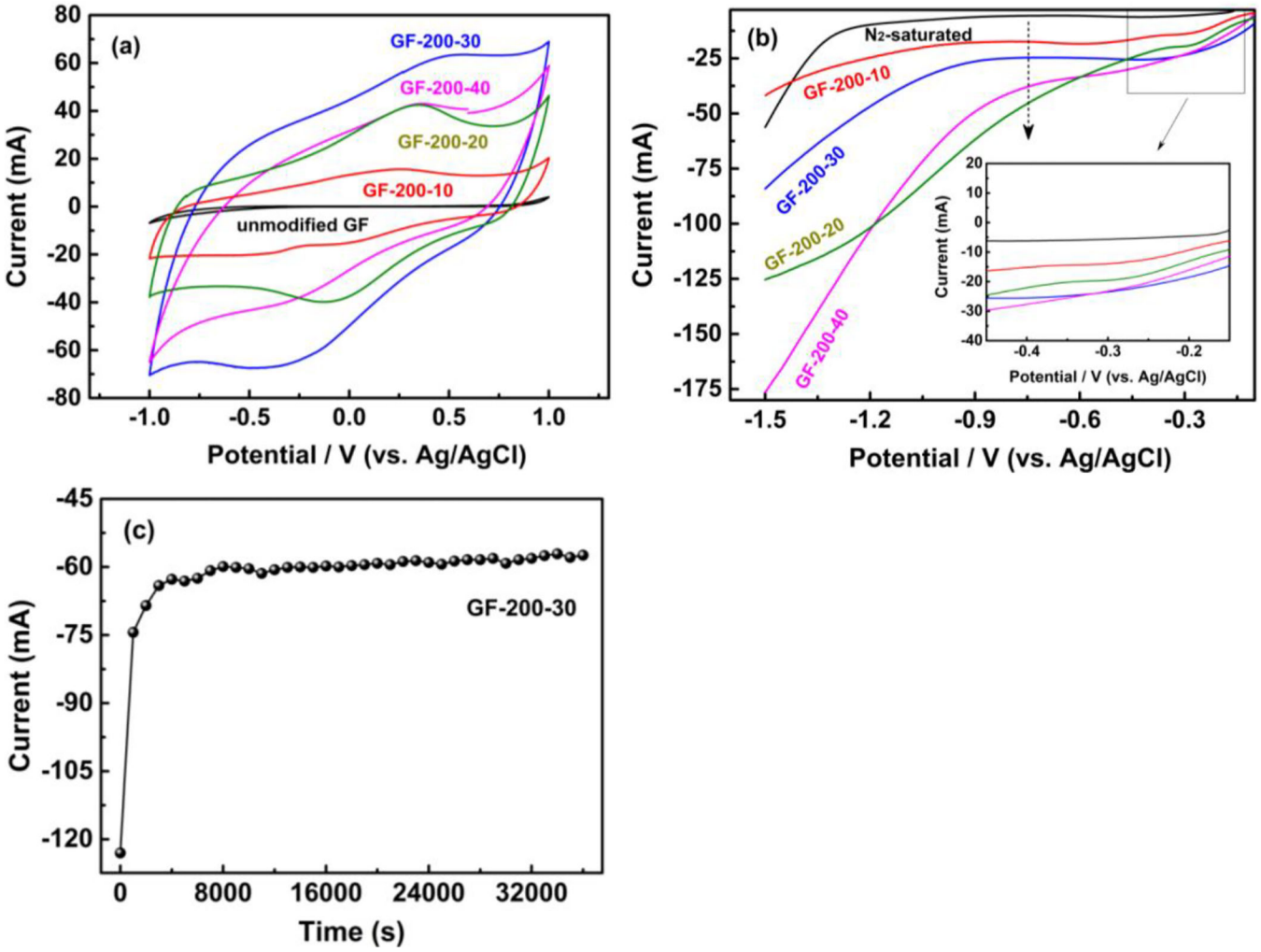

Figure 2.

Electrochemical characterization of unmodified and modified GF electrodes. **(a)** CV curves recorded at 20 mV/s in the scan range of −1.0 to 1.0 V in 50 mM Na_2SO_4 solution, **(b)** LSV curves recorded at 10 mV/s in the scan range of 0 to −1.5 V in 50 mM Na_2SO_4 solution in N_2 and O_2 saturated solution, and (c) chronoamperometry of GF-200–30 electrode in O_2-saturated 50 mM Na_2SO_4 electrolyte at neutral pH (applied potential: −0.9 V vs. Ag/AgCl).

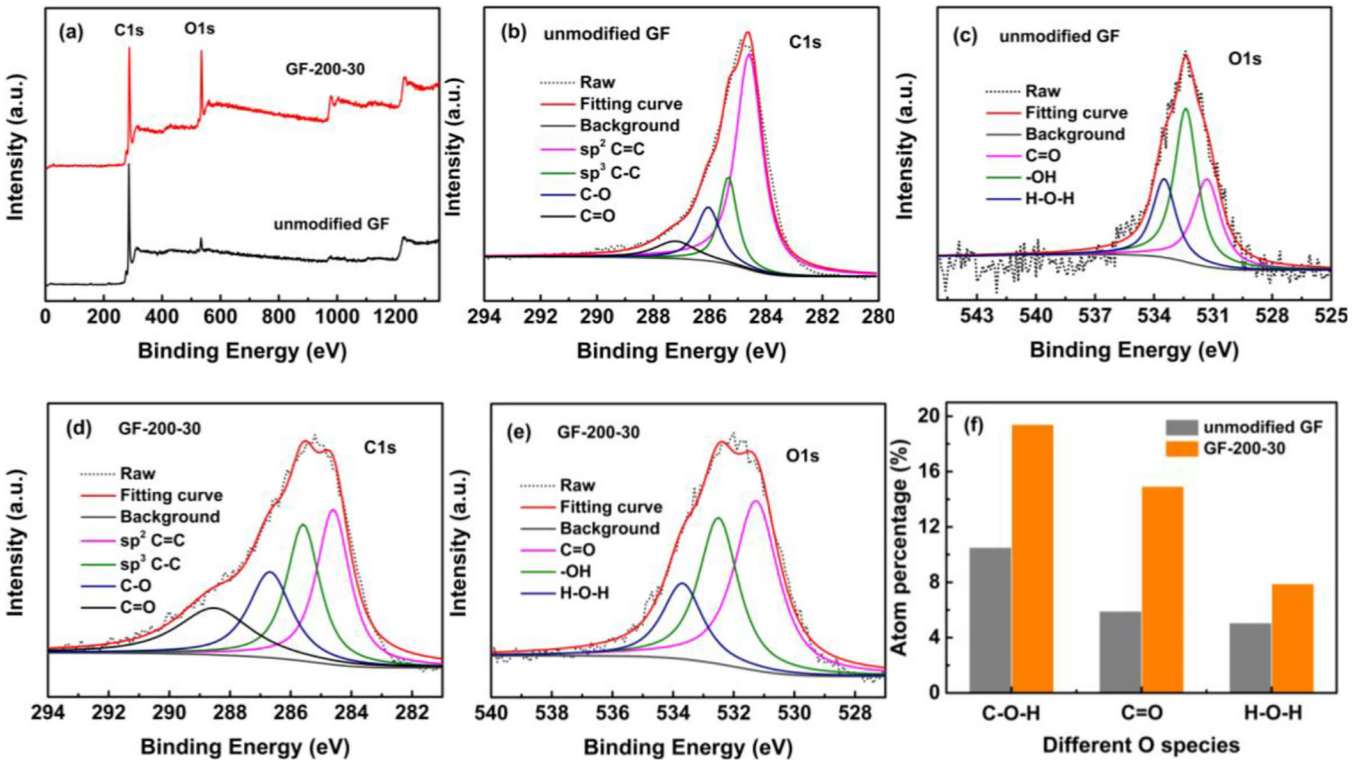

Figure 3.

XPS characterization of the unmodified GF and GF-200–30. (a) XPS survey spectra of unmodified GF and GF-200–30, XPS C1s peaks (b) and O1s peaks (c) of unmodified GF, XPS C1s peaks (d) and O1s peaks (e) of GF-200–30, and (f) atomic percentage distribution of the three major O species of unmodified GF and GF-200–30.

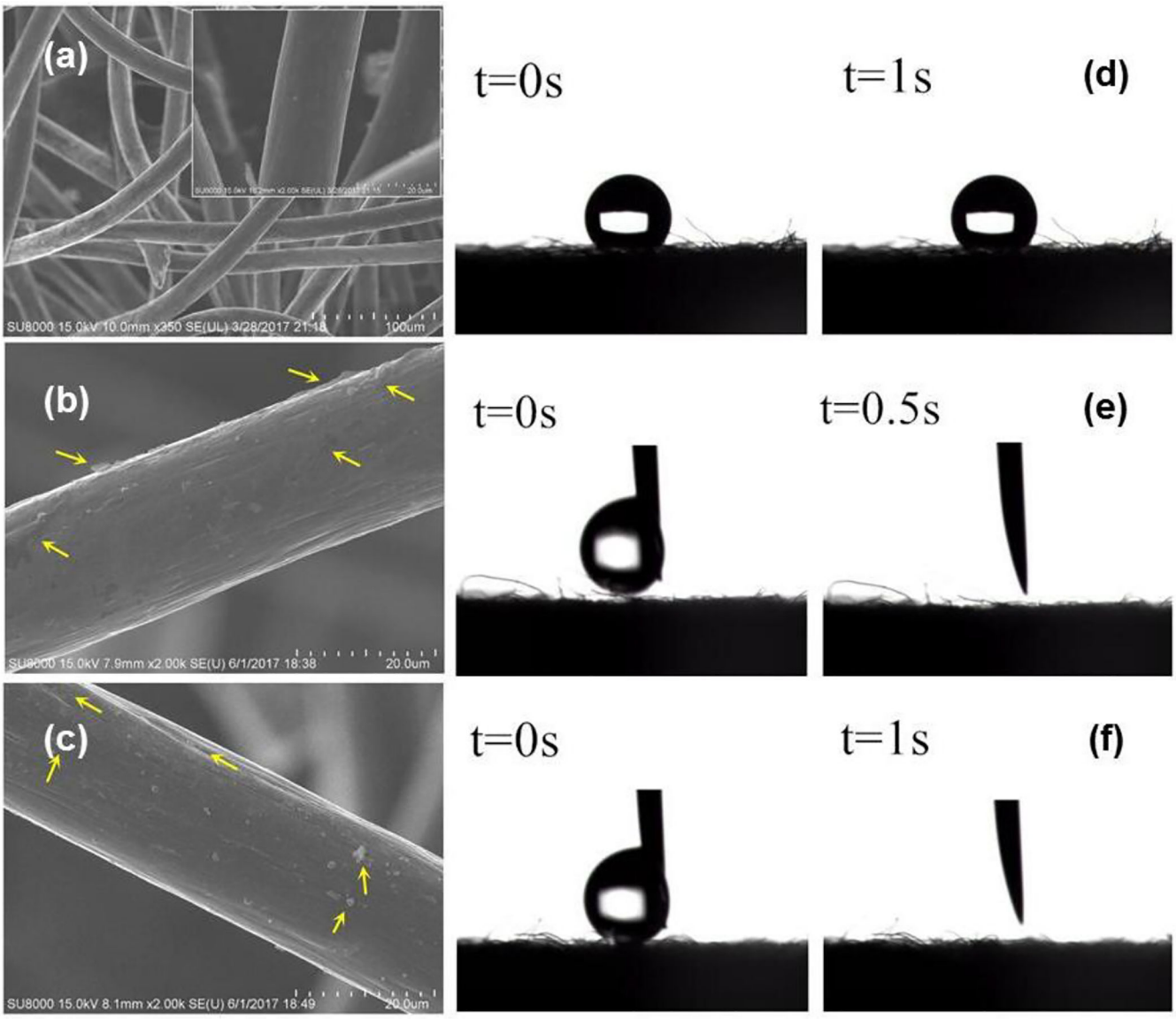

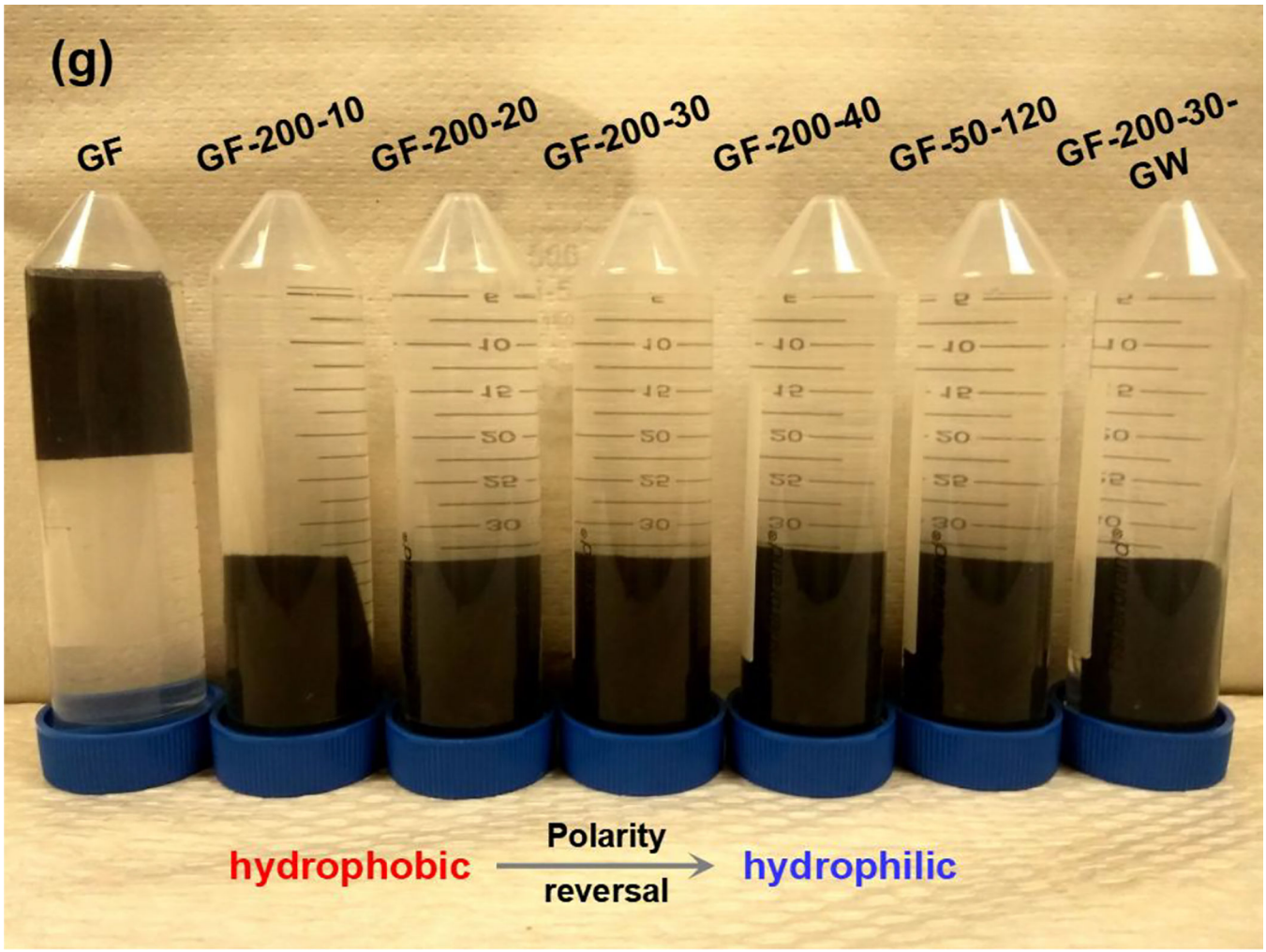

Figure 4.

SEM images of unmodified GF **(a)**, GF-200–30 **(b)**, and GF-200–30-GW **(c)**. Contact angle of GF **(d)** GF-200–30 **(e)**, and GF-200–30-GW **(f)**. **(g)** Photo of the unmodified and modified GF in 50 mM Na_2SO_4 electrolyte and simulated groundwater.

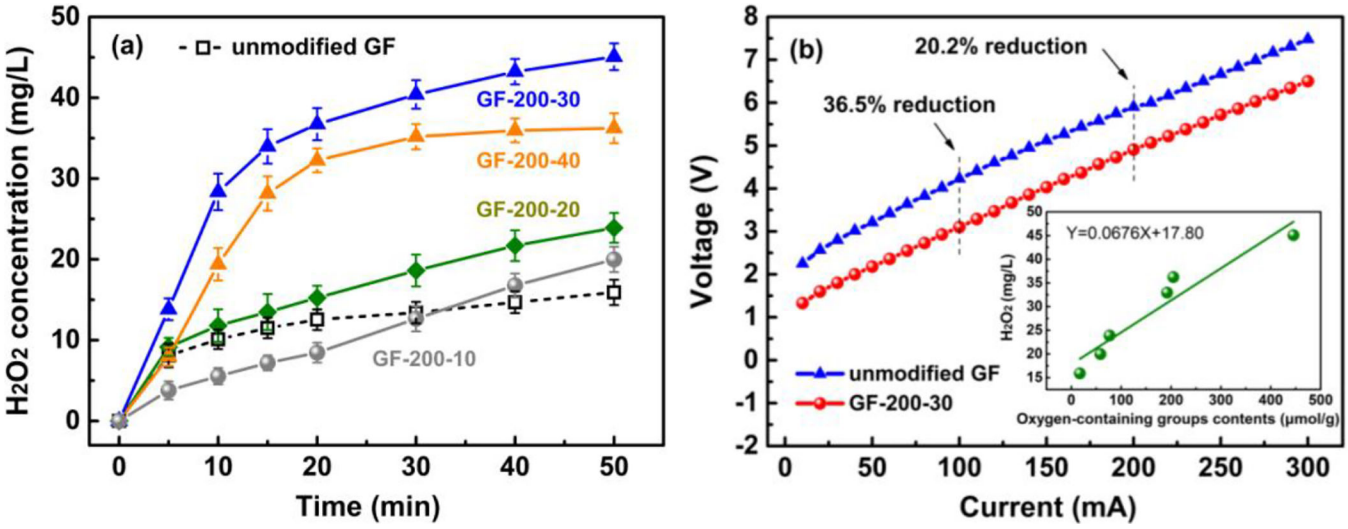

Figure 5.

(a) Influence of electrooxidation extent on H_2O_2 production; **(b)** profile of voltage under different currents for unmodified and modified GF electrodes; inner figure shows the linear correlation between the contents of oxygen-containing groups (measured by NaOH uptake method) and H_2O_2 concentration after 60 min. Conditions for modification: 180 mL, 50 mM Na_2SO_4, without stirring, pH of 7, extent of 480, 960, 1440, and 1920 C/g. Conditions for H_2O_2 production: 180 mL, 50 mM Na_2SO_4, pH of 7, 100 mA.

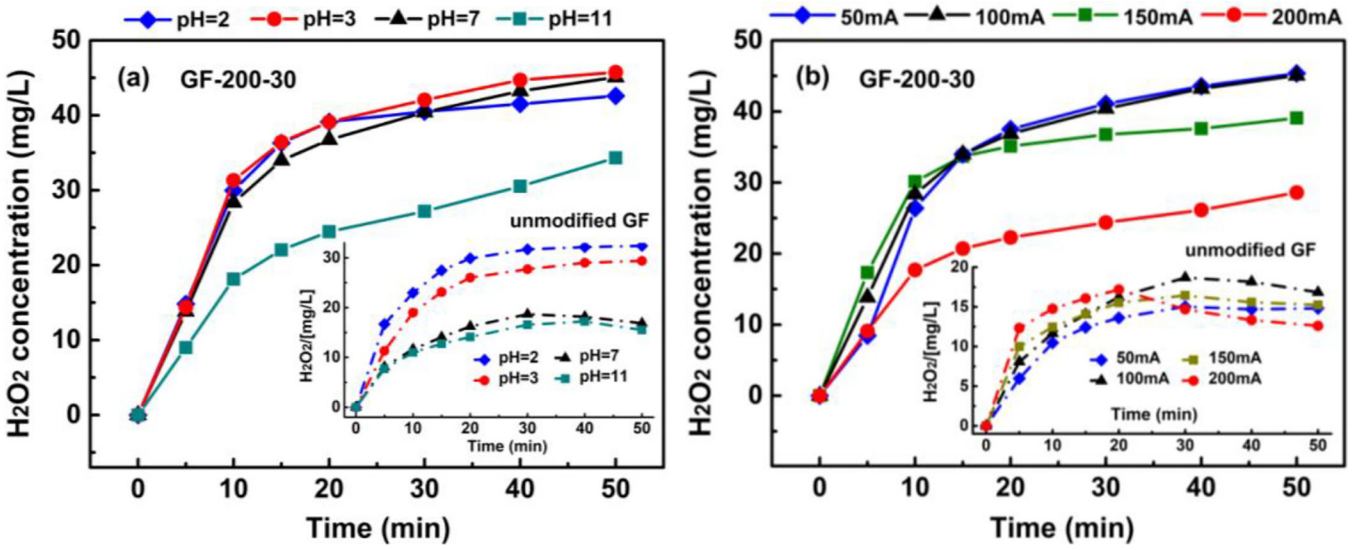

Figure 6.

Influence of pH **(a)** and current **(b)** on H_2O_2 production by unmodified GF (inset figures) and GF-200–30. Conditions: 180 mL, 50 mM Na_2SO_4, pH of 7 (for (b)), 100 mA (for (a)), 350 rpm.

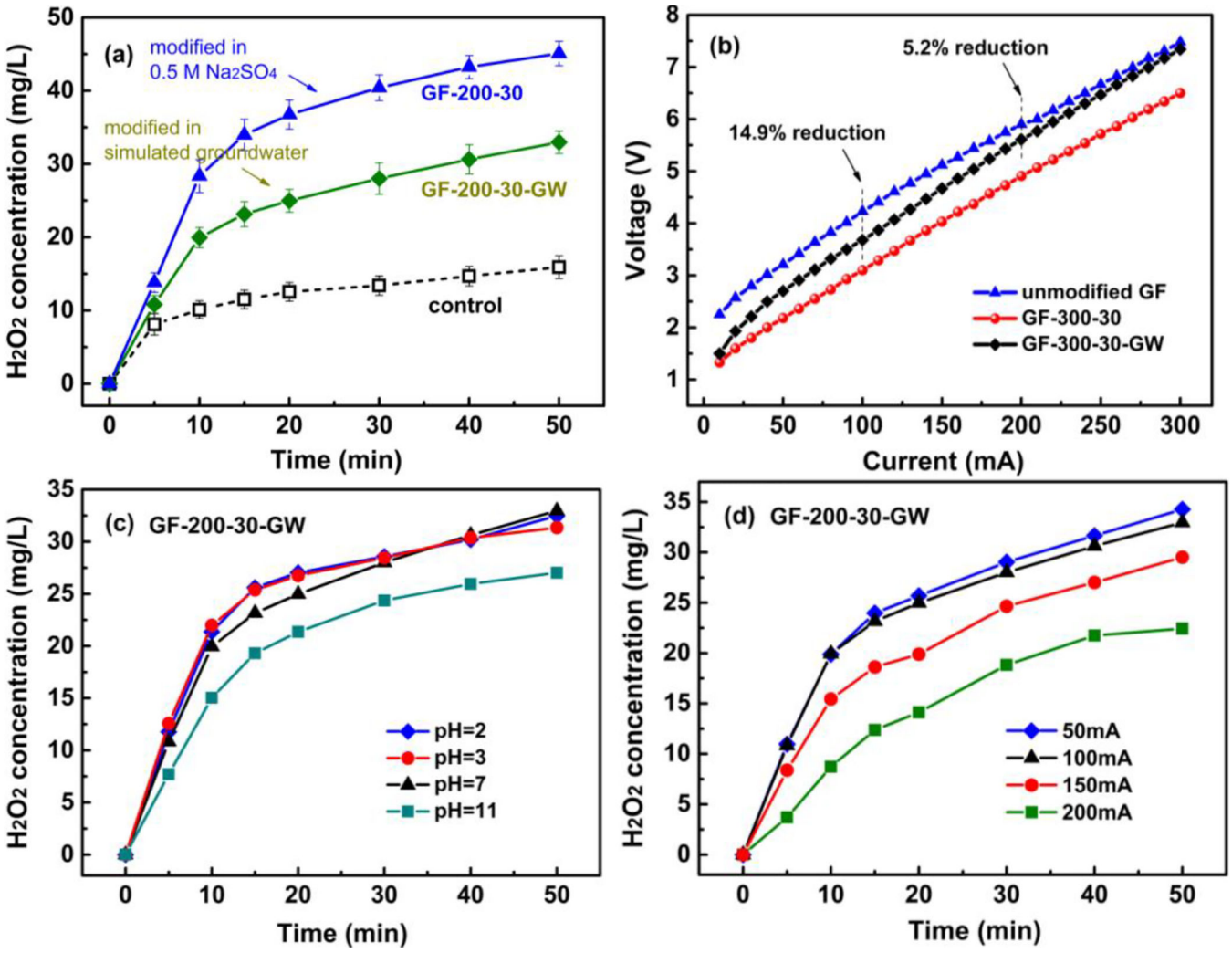

Figure 7.

(a) Comparison of GF modified in simulated groundwater and 50 mM Na_2SO_4 electrolyte for H_2O_2 production. **(b)** Comparison of voltage change for GF modified in simulated groundwater and 50 mM Na_2SO_4 electrolyte. **(c)~(d)** Influence of pH (c) and current (d) on H_2O_2 production by GF-200–30-GW electrode. Conditions for modification: 180 mL, simulated groundwater, without stirring, pH of 7, extent of 1440 C/g (200 mA, 30 min). Conditions for H_2O_2 production: 180 mL, 50 mM Na_2SO_4, pH of 7 (for a,b, and d), 100 mA (for a and c), 350 rpm.

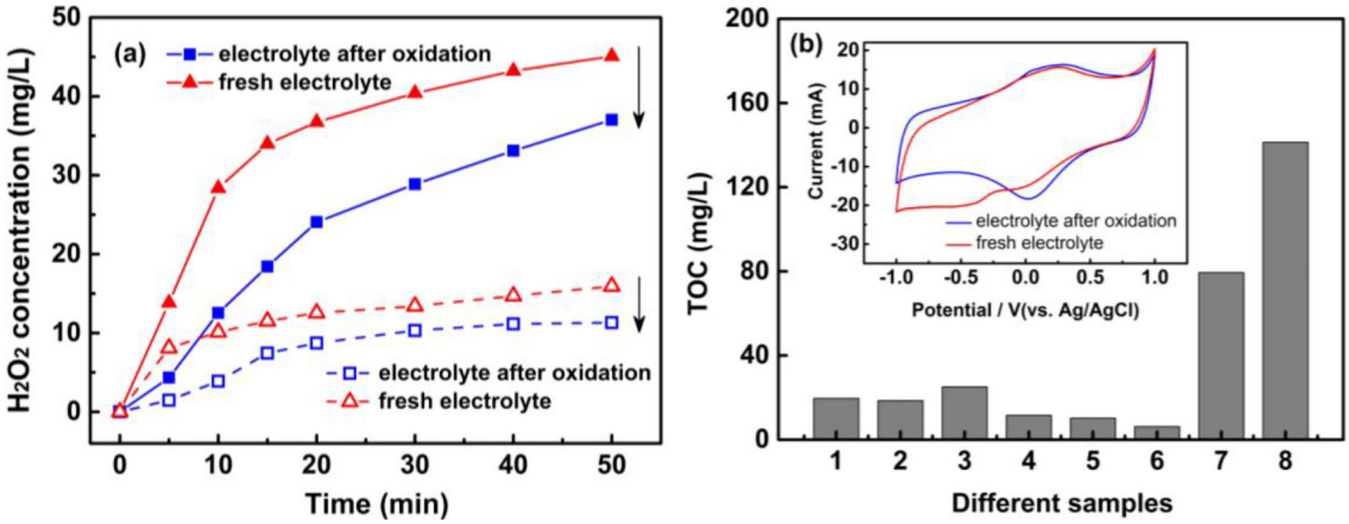

Figure 8.

(a) H_2O_2 generation in residual electrolyte after electrochemical modification under 200 mA for 30 min (modified (solid), unmodified (hollow)); **(b)** TOC in electrolyte after electrooxidation of GF under different parameters; No. 1–3 and 7 were conducted in 50 mM Na_2SO_4 electrolyte, No. 4–6 were conducted in 50 mM Na_2SO_4 electrolyte with polarity reversal by different frequencies, No. 8 was conducted in simulated groundwater (1: GF-200–10, 2: GF-200–20, 3: GF-200–30, 7: GF-200–40, 4: GF-200–30-(“50s+50s”), 5: GF-200–30-(“2min+2min”), 6: GF-200–30-(“10min+10min”), 8: GF-200–30-GW).

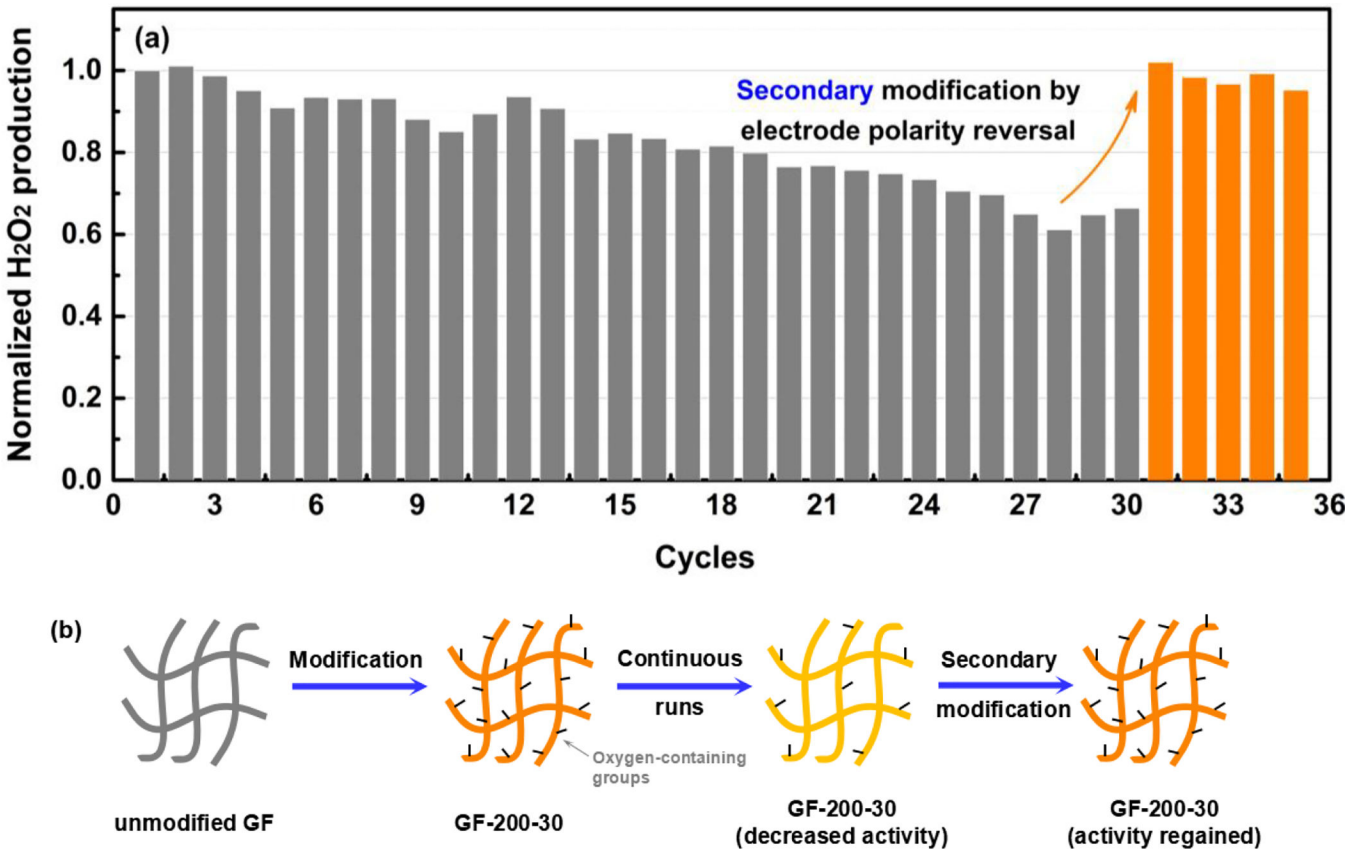

Figure 9.

The cycling performance of GF-200–30 **(a)** and the illustration of surface change of GF-200–30 over continuous operations and secondary modification **(b)**. Conditions for secondary modification: 180 mL, 50 mM Na_2SO_4, without stirring, pH of 7, extent of 1440 C/g (200 mA, 30 min). Conditions for H_2O_2 production: 180 mL, 50 mM Na_2SO_4, pH of 7, 100 mA, 350 rpm.

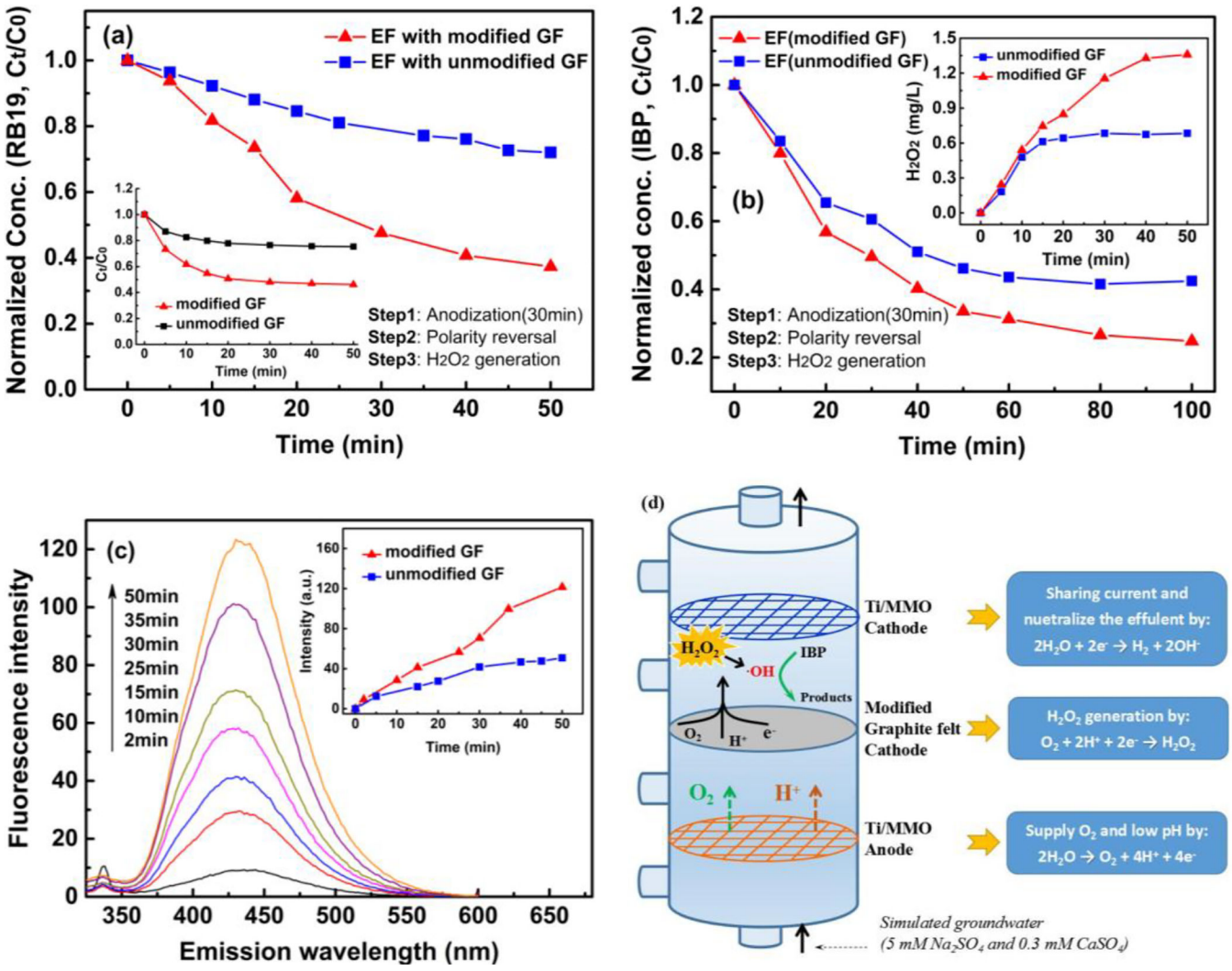

Figure 10.

Normalized concentration of RB19 **(a)** and IBP **(b)** in EF process with unmodified GF and GF-200–30 electrode. The internal figures show adsorption of RB19 by GF **(a)** and profile of H_2O_2 concentration in flow-through reactor **(b)**. **(c)** Comparison of hydroxyl radicals generation in EF process using unmodified GF and GF-200–30 electrode. **(d)** 3-electrode flow-through reactor. Conditions for (a) and (b): initial concentration of RB19 and IBP is 20 mg/L and 10 mg/L, respectively; 10 mg/L Fe^{2+}, pH of 3, 350 rpm, 180 mL, 100 mA (for (a)); flow rate of 3 mL/min, total current of 120 mA with 60 and 60 mA distributed through cathodes 1 and 2 (for (b)). Conditions for (c): 350 rpm, 180 mL, 100 mA, 10 mM benzoic acid, excitation wavelength at 303 nm. The fluorescence spectra represent EF process using GF-200–30 electrode.

Table 1

Conditions reported in the literature for electrooxidation of carbon materials

Materials	Electrolyte	Concentration	Extent of electrooxidation	Ref.
Porous Carbon	K_2SO_4	0.5 M	30, 50 mA-300h	Barton et al., 1997 [40]
Carbon Fibers	KNO_3	1% wt	133~10600 C/g	Yue et al., 1999 [43]
Activated Carbon	NaCl	2% wt	0.2, 0.5, 1 A for 2 h	Berenguer et al., 2012 [34]
Carbon Cloth	KNO_3/HNO_3	0.5 M KNO_3 0.01 M HNO_3	0.2, 0.5, 1 A for 3 h	Tabti et al., 2014 [47]
Graphite Felt	H_2SO_4	5, 10, 20% wt	0~2V at a rate of 10mV/s	Miao et al., 2014 [33]
Graphite Felt	H_2SO_4	1 M	30 mA/cm^2 12 h	Tang et al., 2011 [37]
Graphite Felt	H_2SO_4	1 M	100 mA/cm^2 Different time	Zhang et al., 2013 [38]
Graphite Felt	H_2SO_4	1 M	5–15V For different time	Li et al, 2007 [42]
Carbon Nanofibers	H_2SO_4	5% wt	1.0, 1.2, 1.5, 2.0 V for 30 min	Yoon et al., 2011 [41]

Table 2

The content of surface elements and oxygen-containing groups on the surface of unmodified GF and GF-200–30.

Sample	O/C ratio	C=C, C-C (%)	O (%)	Oxygen-containing groups		
				C-O-H (%)	C=O (%)	H_2O (%)
GF	0.055	78.50	21.50	10.52	5.91	5.07
GF-200–30	0.218	57.87	42.13	19.41	14.93	7.89